

Deformable Registration of Brain Tumor Images via a Statistical Model of Tumor-Induced Deformation

Ashraf Mohamed^{1,2}, Dinggang Shen^{1,2} and Christos Davatzikos^{1,2}

¹ CISST NSF Engineering Research Center,

Department of Computer Science, Johns Hopkins University

² Section for Biomedical Image Analysis, Department of Radiology,

University of Pennsylvania School of Medicine

{ashraf,dgshen,christos}@rad.upenn.edu

Abstract. An approach to deformable registration of three-dimensional brain tumor images to a normal brain atlas is presented. The approach involves the integration of three components: a biomechanical model of tumor mass-effect, a statistical approach to estimate the model's parameters, and a deformable image registration method. Statistical properties of the desired deformation map are first obtained through tumor mass-effect simulations on normal brain images. This map is decomposed into the sum of two components in orthogonal subspaces, one representing inter-individual differences, and the other involving tumor-induced deformation. For a new tumor case, a partial observation of the desired deformation map is obtained via deformable image registration and is decomposed into the aforementioned spaces in order to estimate the mass-effect model parameters. Using this estimate, a simulation of tumor mass-effect is performed on the atlas to generate an image that is more similar to brain tumor image, thereby facilitating the atlas registration process. Results for a real and a simulated tumor case indicate significant reduction in the registration error due to the presented approach as compared to the direct use of deformable image registration.

1 Introduction

Deformable registration of normal brain images into a common stereotactic space makes possible the construction of statistical atlases that are based on collective morphological, functional, and pathological information [1]. Similar atlases constructed from tumor patients' images can act as tools for optimal planning of therapeutic and neuro-surgical approaches that deal with tumors by statistically linking functional, and structural neuroanatomy to variables such as tumor size, location, and grade to the surgical or treatment approach and outcomes [2–5].

A major hurdle preventing the construction of such brain tumor atlases is the unsuitability of currently available deformable registration methods for adapting a tumor-bearing image to the stereotactic space of a normal neuro-anatomy atlas image. This is due to the substantial dissimilarity between the two images

resulting from topological differences, tissue death and resorption, the confounding effects of edema and tissue infiltration, and severe deformation in the vicinity of the tumor beyond natural anatomical variability.

To account for topological differences between the atlas and the patient’s images, Dawant et al. [4] proposed the introduction of a tumor “seed” in the atlas image and relied on image features to drive the registration. Bach Cuadra et al. [5] extended this idea with the use of a radially symmetric model of tumor growth. The lack of a physically realistic model of tumor-induced deformation, as well as the approximate determination of the seed location results in limited accuracy of these approaches for large tumor cases. Kyriacou et al. [2] used a biomechanical model of the deformation caused by tumors to register images of tumor patients to anatomical atlases. However, this approach was only implemented in 2D and relied on a computationally expensive regression procedure to solve the inverse problem of estimating the tumor location in the atlas.

In order to register brain tumor images to a normal anatomical brain atlas, here we present an approach that requires the integration of 3 components. The first, is a biomechanical 3D model for the soft-tissue deformation caused by the bulk tumor and peri-tumor edema. This model is implemented using the finite element (FE) method and is used to generate a number of examples of deformed brain anatomies due to tumors starting from normal brain images. The second component is a statistical model of the desired deformation map which approximates this map via the sum of two components in orthogonal subspaces with different statistical properties. For any particular tumor case that should be registered to the atlas, a partial observation of the desired deformation map is obtained via a deformable image registration method, which is the third component of the presented approach. Based on the constructed statistical model of the deformation, this partial observation is used to estimate the corresponding mass-effect model parameters that would have produced such a deformation. Finally, the desired deformation is obtained by applying the mass-effect model to the atlas image and the use of deformable image registration to match it to the subject’s image. Details of the proposed approach are presented in Sect. 2.

In Sect. 3, we demonstrate our approach on real and simulated tumor cases, and we show that the registration error decreases significantly with our approach compared to the direct use of a readily available image registration method. The paper is concluded with a discussion of future work in Sect. 4.

2 Methods

The proposed approach is explained with the aid of Fig. 1. The subject’s brain B_{SD} includes regions T_{SD} (bulk tumor), and possibly D_{SD} (peri-tumor edema). The main goal of the deformable registration problem is to find the homeomorphism $\chi_f : B_A \setminus T_A \rightarrow B_{SD} \setminus T_{SD}$ which maps points with coordinates \mathbf{X}_A in the atlas image to points with coordinates \mathbf{X}_{SD} in the subject image. Another goal is to identify T_A , which corresponds to brain tissue that is no longer present in the subject’s image (died or invaded by tumor).

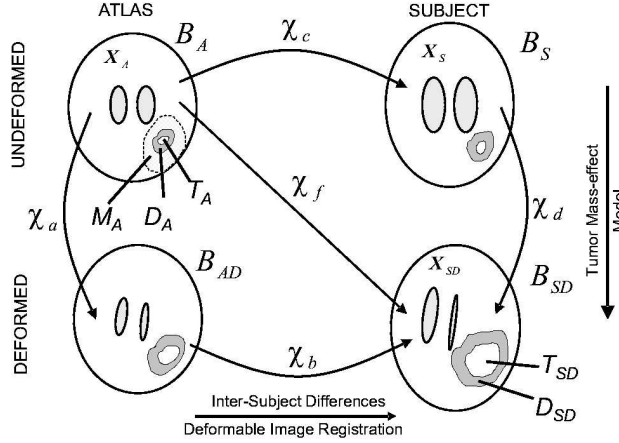


Fig. 1. Illustration of the deformation maps involved in the proposed approach. χ_f is the map from the atlas to a subject's tumor-bearing image. Regions T_{SD} and D_{SD} denote the bulk tumor and edema regions in the subject's images, and T_A , D_A are the corresponding regions in the atlas. χ_c is the mapping from the atlas to the subject's image before tumor mass-effect simulation (B_S is not known for non-simulated cases), and χ_a is that obtained through the simulation of tumor mass-effect. Simulating the tumor mass-effect on the atlas results in χ_a and a deformed atlas image which can then be registered to the deformed subject's image through χ_b .

If an accurate model of the deformation induced by the tumor is available, it can be used to simulate this deformation in the atlas and obtain χ_a , followed by the application of deformable image registration to get χ_b , and therefore $\chi_f = \chi_b \circ \chi_a$. A model of the mass-effect caused by tumor growth is described in Sect. 2.1. Estimates of region T_A as well as the other parameters affecting the model's behavior, such as the extent of peri-tumor edema and the mass-effect of the bulk tumor, are still needed in order to apply this approach. Here, we solve this inverse estimation problem by exploiting the statistical dependency between χ_f and the mass-effect model parameters. Although an approximation of χ_f obtained by the direct application of deformable image registration is incorrect in and around the tumor (region M_A in Fig. 1), the pattern of this deformation outside that region can guide the estimation of the tumor model parameters. In Sect. 2.2, we explain the collection of the statistics on $\chi_f = \chi_d \circ \chi_c$ through tumor mass-effect simulations on images of normal subjects. Estimation of the mass-effect model parameters is explained in Sect. 2.3.

2.1 Tumor Mass-Effect Model

This model is initialized with a 3D normal brain image (free of tumor) and it produces an estimate of the deformation due to the mass-effect of a simulated tumor. We explain the model by assuming that it is applied to the atlas image,

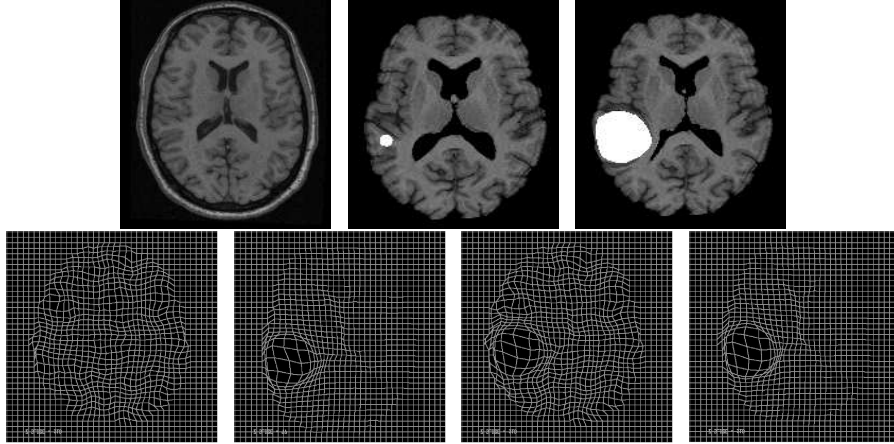


Fig. 2. Illustration of a tumor mass-effect simulation and the associated displacement maps. Upper row (left to right): atlas image, normal subject's MRI with an introduced small tumor, and resulting image after simulation of tumor mass-effect. Lower row (Left to right): displacement map \mathbf{u}_c , displacement map $\chi_d - \mathbf{X}_s$, displacement map \mathbf{u}_f , and displacement map \mathbf{u}_d .

although as explained later, the model may also be applied to other normal images for statistical training.

With the assumption that the mass-effect is due to the bulk tumor and the peri-tumor edema only, regions T_A and D_A are defined in the undeformed (normal) atlas image. These correspond to the bulk tumor and peri-tumor edema regions in the deformed atlas at the end of the simulation. Although these regions are highly variable for different tumor cases and are not known in general, here for tractability, we assume that T_A and D_A are spherical and concentric with center \mathbf{c}_t and radii r_t and r_d respectively. It is important to note that this does not restrict our approach to dealing with spherical tumors only since final simulated tumors need not be spherical (see Fig. 2) and also these regions are later refined through the deformable image registration component of our approach.

Brain tissue swelling due to edema is restricted to white matter in D_A and a volume expansion of 250% is used. Swelling is simulated by analogy to thermal expansion. We further assume that the expansive force of the bulk tumor may be approximated with a pressure P normal to the boundary of T_A [6]. With these assumptions, appending the necessary boundary conditions at the falx cerebri and the brain surface [7], and using the material constitutive model suggested in [8] for brain tissues, a mechanical problem is formulated and solved using the FE method. More details on this tumor mass-effect model can be found in [9]. The model parameters are collectively referred to by $\Theta \equiv (\mathbf{c}_t, r_t, r_d, P)$. The values of these parameters are not known for a real tumor case, but are estimated using the statistical model of the deformation explained next.

2.2 Statistical Model Training

The goal of this step is to create a statistical model for the deformation χ_f that will aid in the estimation of Θ for a particular tumor image. First, the deformation maps $\chi_{c_i}, i = 1, \dots, n_s$ between the atlas and MRI images of n_s normal subjects are obtained using a deformable image registration approach [10]. Simulations of the mass-effect of tumor growth are then conducted for each subject i for values $\Theta_j, j = 1, \dots, n_m$ covering a range of the model parameters to produce the deformations $\chi_{d_{i,j}}, i = 1, \dots, n_s, j = 1, \dots, n_m$.

A problem preventing the collection of statistics on $\chi_{d_{i,j}}$ directly is that the domains of these maps are different for different values of i and j . This precludes the point-to-point comparison of these deformation maps. To overcome this problem, for all tumor model simulations, regions T_{A_j} and D_{A_j} are defined in the atlas space based on Θ_j and mapped to each subject's space via $\chi_{c_i}, i = 1, \dots, n_s$. Next, for $\mathbf{X}_A \in B_A \setminus T_{A_j}, i = 1, \dots, n_s, j = 1, \dots, n_m$, we define

$$\mathbf{u}_{d_{i,j}}(\mathbf{X}_A) \equiv \chi_{f_{i,j}}(\mathbf{X}_A) - \chi_{c_i}(\mathbf{X}_A) = \chi_{d_{i,j}}(\chi_{c_i}(\mathbf{X}_A)) - \chi_{c_i}(\mathbf{X}_A) \quad (1)$$

$$\mathbf{u}_{c_i}(\mathbf{X}_A) \equiv \chi_{c_i}(\mathbf{X}_A) - \mathbf{X}_A \quad (2)$$

$$\mathbf{u}_{f_{i,j}}(\mathbf{X}_A) \equiv \chi_{f_{i,j}}(\mathbf{X}_A) - \mathbf{X}_A = \mathbf{u}_{c_i}(\mathbf{X}_A) + \mathbf{u}_{d_{i,j}}(\mathbf{X}_A). \quad (3)$$

For different $i = 1, \dots, n_s$, but the same $j = 1, \dots, n_m$, the domains of $\mathbf{u}_{d_{i,j}}$ are the same. An example of a tumor model simulation and the involved displacement maps is shown in Fig. 2.

We construct discrete versions of the displacement maps \mathbf{u}_{c_i} and $\mathbf{u}_{d_{i,j}}$ by sampling their cartesian components for all voxels in the atlas in $B_A \setminus M_A$ to yield vectors \mathbf{U}_{c_i} and $\mathbf{U}_{d_{i,j}}$ respectively. Assuming that $\mathbf{U}_{c_i}, i = 1, \dots, n_s$ are independent realizations of a Gaussian random vector, principal component analysis (PCA) is applied to these vectors to yield the mean $\boldsymbol{\mu}_c$ and the matrix \mathbf{V}_c whose columns are eigenvectors corresponding to the first m_c principal components ($m_c \leq n_s - 1$). Next, we compute the component of $\mathbf{U}_{d_{i,j}}$ in the subspace orthogonal to the columns of \mathbf{V}_c as

$$\mathbf{U}'_{d_{i,j}} = \mathbf{U}_{d_{i,j}} - \mathbf{V}_c \mathbf{V}_c^T \mathbf{U}_{d_{i,j}}. \quad (4)$$

We further assume that, for each $j, \mathbf{U}'_{d_{i,j}}, i = 1, \dots, n_s$ are independent realizations of a Gaussian random vector and we perform PCA on these vectors to yield the mean $\boldsymbol{\mu}_{d_j}$ and the matrices \mathbf{V}_{d_j} whose columns are eigenvectors corresponding to the first m_{d_j} principal components ($m_{d_j} \leq n_s - 1$). Now, we can approximate the discrete displacement map \mathbf{U}_f between the atlas and a subject with a simulated tumor with parameters $\Theta_j, j = 1, \dots, n_m$ as follows:

$$\mathbf{U}_f \approx \boldsymbol{\mu}_c + \mathbf{V}_c \mathbf{a} + \boldsymbol{\mu}_{d_j} + \mathbf{V}_{d_j} \mathbf{b}_j. \quad (5)$$

The vectors \mathbf{a} and \mathbf{b}_j each follows a Gaussian distribution with decorrelated components, with that of \mathbf{b}_j denoted by $f_j(\mathbf{b}_j)$.

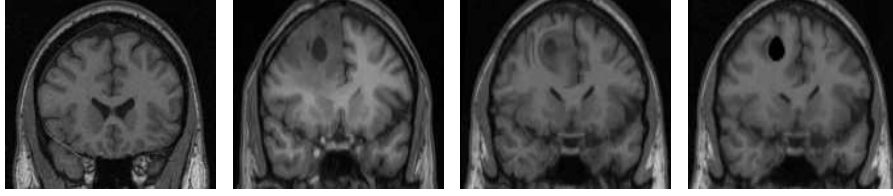


Fig. 3. Results of applying the proposed approach to register the real tumor case to the atlas. Left to right: Atlas image, subject's image, warped atlas image in the subject's space with the use of deformable registration directly between the two images, and the warped atlas image in the subject's space with the use of the proposed approach.

2.3 Statistical Estimation

Given an approximate deformation map $\tilde{\chi}_f$ (between a real tumor patient's images and the atlas) obtained by the direct use of deformable image registration, the goal of the methods presented here is to obtain an estimate $\hat{\Theta}$ of the tumor model parameters. The displacement map $\tilde{\mathbf{u}}_f$ defined in a similar manner to eqn. 3 is also discretized over all the atlas voxels in $B_A \setminus M_A$ and represented by a vector $\tilde{\mathbf{U}}_f$. Owing to the orthogonality of \mathbf{V}_{d_j} to \mathbf{V}_c for all j , we can compute the component of this displacement that is caused by the tumor by projection as

$$\tilde{\mathbf{U}}_d = \tilde{\mathbf{U}}_f - \boldsymbol{\mu}_c - \mathbf{V}_c \tilde{\mathbf{a}}, \quad (6)$$

where $\tilde{\mathbf{a}} = \mathbf{V}_c^T (\tilde{\mathbf{U}}_f - \boldsymbol{\mu}_c)$. The likelihood of having $\tilde{\mathbf{U}}_d$ be generated with tumor model parameters Θ_j is defined as $L_j \equiv f_j(\tilde{\mathbf{b}}_j)$, where $\tilde{\mathbf{b}}_j = \mathbf{V}_{d,j}^T (\tilde{\mathbf{U}}_d - \boldsymbol{\mu}_{d,j})$, for $j = 1, \dots, n_m$. We estimate the tumor model parameters as

$$\hat{\Theta} = \left(\sum_{j=1}^{n_m} L_j \Theta_j \right) / \left(\sum_{j=1}^{n_m} L_j \right) \quad (7)$$

3 Experiments and Results

Results of applying the approach described above are reported here for two cases. The first is an MRI of patient with a glioma and a large region of peri-tumor edema. The second is a simulated tumor image obtained by applying the mass-effect model described in Sect. 2.1 to an MRI of a normal subject. All images used are T1-weighted MRI. The atlas image dimensions are 256x256x198 and a voxel size of 1x1x1mm. Other images used are of dimensions 256x256x124 and voxel size 0.9375x0.9375x1.5mm.

The FE tumor mass-effect model simulations are the most computationally intensive step of the presented approach. In order to make the statistical training step tractable, we performed tumor simulations on $n_s = 20$ MRI brain images of normal subjects. For each subject $n_m = 64$ simulations were performed with 2 values of each of the six model parameters covering the range expected for the real tumor case. The parameter values were $r_t \in \{3, 5\}mm$, $r_d \in \{20, 27\}mm$,

	Minimum	Mean	Maximum	Standard Deviation
RT no Model, mm	1.06	8.70	24.87	6.19
RT with Model, mm	0.47	3.69	7.19	1.83
ST no Model, mm	2.54	6.39	10.91	2.62
ST with Model, mm	0.61	3.90	7.79	2.01

Table 1. Deformable registration error statistics for landmark points in the real tumor (RT) and simulated tumor (ST) cases. For each case, the errors are provided for the direct deformable image registration to the atlas (No Model), and the registration using the approach described in this paper (with Model). 21 landmark points were used for RT and 25 were used for ST.

$P \in \{2, 5\}kPa$ and corners of a cube in the atlas for the simulated tumor center locations. For the results reported here, all principal components of the displacement \mathbf{U}_c were retained and we used $m_{d_j} = 1, j = 1, \dots, n_m$.

In Fig. 3, the result of applying our approach to the real tumor subject is demonstrated. With the use of deformable registration to directly register the (normal) atlas image to the subject’s MRI, the warping result is inaccurate in the tumor area. Gray matter from the right cingulate region and adjacent cortical CSF in the atlas were stretched to match the intensity of the tumor and the surrounding edema in the patient’s image. The estimated tumor model parameters were $\hat{\mathbf{c}}_t=(109, 86, 126)$, $\hat{r}_t=3.9mm$, $\hat{r}_d=24mm$ and $\hat{P}=3.55kPa$.

In order to quantitatively assess the improvement in the registration accuracy due to the proposed model, 21 landmark points were selected around the tumor area in the subject and corresponding points were identified by an expert in the atlas. The point coordinates were mapped through the resulting transformation with direct deformable registration and with our approach and the results are presented in Tab. 1. The maximum error was reduced by 71% by the use of our approach while the mean error was reduced by 57.6%.

Similar deformable registration experiments were performed for a simulated tumor case based on an MRI scan of a normal subject. The simulation parameters were $\mathbf{c}_t=(106, 86, 128)$, $r_t=4.5mm$, $r_d=21mm$ and $P=4.5kPa$. Using the approach described above, the estimated values of these parameters were $\hat{\mathbf{c}}_t=(109, 85, 128)$, $\hat{r}_t=4.1mm$, $\hat{r}_d=23mm$ and $\hat{P}=3.6kPa$. To evaluate the registration error in this case, 25 points were selected arbitrarily in the area around the simulated tumor, and their corresponding coordinates (found through $\chi_d \circ \chi_c$ which is available in this case) were computed in the atlas image and treated as ground truth. The errors for the direct deformable registration and that obtained by the proposed approach are also presented in Tab. 1. The maximum error was reduced by 29% using the proposed approach and the corresponding average error was reduced by 39%.

4 Discussion and Future Work

We introduced an approach for deformable registration of atlas to brain tumor images. The approach utilizes a 3D biomechanical FE model of tumor-induced deformation to introduce and simulate the tumor in the atlas followed by the use of a readily available deformable image registration approach. To solve the

inverse problem of determining the model parameters, we proposed a statistical approach that relies on the decomposition of the desired deformation map into the sum of two maps defined on the same domain, but with different statistical properties that are learned via PCA from a number of training samples. These maps are modeled via two orthogonal subspaces which allows the estimation of the tumor model parameters via projection of a rough estimate of the required deformation map on the subspace representing tumor induced-deformation.

The results of applying the proposed approach on a real tumor case and a simulated one indicate significant reduction in the registration error. These experiments should be regarded as a proof-of-concept study. More validation experiments are need to asses the viability of the proposed approach for a variety of tumor cases of different grades, types and sizes. In addition, the sensitivity of the statistical estimator of the model parameters to the number of used principal components and the number of training samples also will be investigated.

Acknowledgments

The authors would like to thank Dr. Nick Fox at the University College London, UK for providing the tumor patient's images. This work was supported in part by the National Science Foundation under Engineering Research Center grant EEC9731478, and by the National Institutes of Health grant R01NS42645.

References

1. Davatzikos, C.: Spatial transformation and registration of brain images using elastically deformable models. *CVIU, Spec. iss. on Medical Imaging* **66** (1997) 207–222
2. Kyriacou, S.K., Davatzikos, C., Zinreich, S.J., Bryan, R.N.: Nonlinear elastic registration of brain images with tumor pathology using a biomechanical model. *IEEE Trans. Med. Imag.* **18** (1999) 580–592
3. Mohamed, A., Kyriacou, S.K., Davatzikos, C.: A statistical approach for estimating brain tumor induced deformation. *Proc. of IEEE Workshop on MMBIA* (2001) 52–59
4. Dawant, B.M., Hartmann, S.L., Pan, S., Gadamsetty, S.: Brain atlas deformation in the presence of small and large space-occupying tumors. *Computer Aided Surgery* **7** (2002) 1–10
5. Cuadra, M.B., Pollo, C., Bardera, A., Cuisenaire, O., Villemure, J.G., Thiran, J.P.: Atlas-based segmentation of pathological MR brains using a model of lesion growth. *IEEE Trans. Med. Imag.* **23** (2004) 1301–1314
6. Wasserman, R., Acharya, R.: A patient-specific in vivo tumor model. *Mathematical Biosciences* **136** (1996) 111–140
7. Miga, M., Paulsen, K., Kennedy, F.E., Hartov, A., Roberts, D.: Model-updated image-guided neurosurgery using the finite element method: Incorporation of the falx cerebri. In: *MICCAI 1999*. (1999)
8. Miller, K., Chinzei, K.: Mechanical properties of brain tissue in tension. *Journal of Biomechanics* **35** (2002) 483–490
9. Mohamed, A., Davatzikos, C.: Finite element modeling of brain tumor mass-effect from 3D medical images. In: *Proceedings of MICCAI 2005*. (2005)
10. Shen, D., Davatzikos, C.: HAMMER: Hierarchical attribute matching mechanism for elastic registration. *IEEE Trans. Med. Imag.* **21** (2002) 1421–1439